

PDF hosted at the Radboud Repository of the Radboud University Nijmegen

The following full text is a preprint version which may differ from the publisher's version.

For additional information about this publication click this link.

<http://hdl.handle.net/2066/124902>

Please be advised that this information was generated on 2017-12-05 and may be subject to change.

An upper limit on the branching ratio for τ decays into seven charged particles

The OPAL Collaboration

Abstract

We have searched for decays of the τ lepton into seven or more charged particles, using data collected with the OPAL detector from 1990 to 1995 in e^+e^- collisions at $\sqrt{s} \approx M_Z$. No candidate events were found and an upper limit on the branching ratio for τ decays into seven charged particles of 1.8×10^{-5} at the 95% confidence level was determined.

(Submitted to Physics Letters B)

The OPAL Collaboration

K. Ackerstaff⁸, G. Alexander²³, J. Allison¹⁶, N. Altekamp⁵, K.J. Anderson⁹, S. Anderson¹², S. Arcelli², S. Asai²⁴, D. Axen²⁹, G. Azuelos^{18,a}, A.H. Ball¹⁷, E. Barberio⁸, R.J. Barlow¹⁶, R. Bartoldus³, J.R. Batley⁵, S. Baumann³, J. Bechtluft¹⁴, C. Beeston¹⁶, T. Behnke⁸, A.N. Bell¹, K.W. Bell²⁰, G. Bella²³, S. Bentvelsen⁸, P. Berlich¹⁰, S. Bethke¹⁴, O. Biebel¹⁴, A. Biguzzi⁵, S.D. Bird¹⁶, V. Blobel²⁷, I.J. Bloodworth¹, J.E. Bloomer¹, M. Bobinski¹⁰, P. Bock¹¹, D. Bonacorsi², M. Boutemour³⁴, B.T. Bouwens¹², S. Braibant¹², L. Brigliadori², R.M. Brown²⁰, H.J. Burckhart⁸, C. Burgard⁸, R. Bürgin¹⁰, P. Capiluppi², R.K. Carnegie⁶, A.A. Carter¹³, J.R. Carter⁵, C.Y. Chang¹⁷, D.G. Charlton^{1,b}, D. Chrisman⁴, P.E.L. Clarke¹⁵, I. Cohen²³, J.E. Conboy¹⁵, O.C. Cooke¹⁶, M. Cuffiani², S. Dado²², C. Dallapiccola¹⁷, G.M. Dallavalle², S. De Jong¹², L.A. del Pozo⁴, K. Desch³, M.S. Dixit⁷, E. do Couto e Silva¹², M. Doucet¹⁸, E. Duchovni²⁶, G. Duckeck³⁴, I.P. Duerdoth¹⁶, D. Eatough¹⁶, J.E.G. Edwards¹⁶, P.G. Estabrooks⁶, H.G. Evans⁹, M. Evans¹³, F. Fabbri², M. Fantì², A.A. Faust³⁰, F. Fiedler²⁷, M. Fierro², H.M. Fischer³, I. Fleck⁸, R. Folman²⁶, D.G. Fong¹⁷, M. Foucher¹⁷, A. Fürtjes⁸, D.I. Futyan¹⁶, P. Gagnon⁷, J.W. Gary⁴, J. Gascon¹⁸, S.M. Gascon-Shotkin¹⁷, N.I. Geddes²⁰, C. Geich-Gimbel³, T. Geralis²⁰, G. Giacomelli², P. Giacomelli⁴, R. Giacomelli², V. Gibson⁵, W.R. Gibson¹³, D.M. Gingrich^{30,a}, D. Glenzinski⁹, J. Goldberg²², M.J. Goodrick⁵, W. Gorn⁴, C. Grandi², E. Gross²⁶, J. Grunhaus²³, M. Gruwé⁸, C. Hajdu³², G.G. Hanson¹², M. Hansroul⁸, M. Hapke¹³, C.K. Hargrove⁷, P.A. Hart⁹, C. Hartmann³, M. Hauschild⁸, C.M. Hawkes⁵, R. Hawkings²⁷, R.J. Hemingway⁶, M. Herndon¹⁷, G. Herten¹⁰, R.D. Heuer⁸, M.D. Hildreth⁸, J.C. Hill⁵, S.J. Hillier¹, T. Hilse¹⁰, P.R. Hobson²⁵, R.J. Homer¹, A.K. Honma^{28,a}, D. Horváth^{32,c}, R. Howard²⁹, D.E. Hutchcroft⁵, P. Igo-Kemenes¹¹, D.C. Imrie²⁵, M.R. Ingram¹⁶, K. Ishii²⁴, A. Jawahery¹⁷, P.W. Jeffreys²⁰, H. Jeremie¹⁸, M. Jimack¹, A. Joly¹⁸, C.R. Jones⁵, G. Jones¹⁶, M. Jones⁶, U. Jost¹¹, P. Jovanovic¹, T.R. Junk⁸, D. Karlen⁶, V. Kartvelishvili¹⁶, K. Kawagoe²⁴, T. Kawamoto²⁴, R.K. Keeler²⁸, R.G. Kellogg¹⁷, B.W. Kennedy²⁰, J. Kirk²⁹, A. Klier²⁶, S. Kluth⁸, T. Kobayashi²⁴, M. Kobel¹⁰, D.S. Koetke⁶, T.P. Kokott³, M. Kolrep¹⁰, S. Komamiya²⁴, T. Kress¹¹, P. Krieger⁶, J. von Krogh¹¹, P. Kyberd¹³, G.D. Lafferty¹⁶, R. Lahmann¹⁷, W.P. Lai¹⁹, D. Lanske¹⁴, J. Lauber¹⁵, S.R. Lautenschlager³¹, J.G. Layter⁴, D. Lazic²², A.M. Lee³¹, E. Lefebvre¹⁸, D. Lellouch²⁶, J. Letts¹², L. Levinson²⁶, S.L. Lloyd¹³, F.K. Loebinger¹⁶, G.D. Long²⁸, M.J. Losty⁷, J. Ludwig¹⁰, A. Macchiolo², A. Macpherson³⁰, M. Mannelli⁸, S. Marcellini², C. Markus³, A.J. Martin¹³, J.P. Martin¹⁸, G. Martinez¹⁷, T. Mashimo²⁴, P. Mättig³, W.J. McDonald³⁰, J. McKenna²⁹, E.A. Mckigney¹⁵, T.J. McMahon¹, R.A. McPherson⁸, F. Meijers⁸, S. Menke³, F.S. Merritt⁹, H. Mes⁷, J. Meyer²⁷, A. Michelini², G. Mikenberg²⁶, D.J. Miller¹⁵, A. Mincer^{22,e}, R. Mir²⁶, W. Mohr¹⁰, A. Montanari², T. Mori²⁴, M. Morii²⁴, U. Müller³, K. Nagai²⁶, I. Nakamura²⁴, H.A. Neal⁸, B. Nellen³, R. Nisius⁸, S.W. O’Neale¹, F.G. Oakham⁷, F. Odoric², H.O. Ogren¹², N.J. Oldershaw¹⁶, M.J. Oreglia⁹, S. Orito²⁴, J. Pálkás^{33,d}, G. Pásztor³², J.R. Pater¹⁶, G.N. Patrick²⁰, J. Patt¹⁰, M.J. Pearce¹, S. Petzold²⁷, P. Pfeifenschneider¹⁴, J.E. Pilcher⁹, J. Pinfold³⁰, D.E. Plane⁸, P. Poffenberger²⁸, B. Poli², A. Posthaus³, H. Przysieznik³⁰, D.L. Rees¹, D. Rigby¹, S. Robertson²⁸, S.A. Robins²², N. Rodning³⁰, J.M. Roney²⁸, A. Rooke¹⁵, E. Ros⁸, A.M. Rossi², M. Rosvick²⁸, P. Routenburg³⁰, Y. Rozen²², K. Runge¹⁰, O. Runolfsson⁸, U. Ruppel¹⁴, D.R. Rust¹², R. Rylko²⁵, K. Sachs¹⁰, T. Saeki²⁴, E.K.G. Sarkisyan²³, C. Sbarra²⁹, A.D. Schaile³⁴, O. Schaile³⁴, F. Scharf³, P. Scharff-Hansen⁸, P. Schenk³⁴, J. Schieck¹¹, P. Schleper¹¹, B. Schmitt⁸, S. Schmitt¹¹, A. Schöning⁸, M. Schröder⁸, H.C. Schultz-Coulon¹⁰, M. Schulz⁸, M. Schumacher³, C. Schwick⁸, W.G. Scott²⁰, T.G. Shears¹⁶, B.C. Shen⁴, C.H. Shepherd-Themistocleous⁸, P. Sherwood¹⁵, G.P. Siroli², A. Sittler²⁷, A. Skillman¹⁵, A. Skuja¹⁷, A.M. Smith⁸, G.A. Snow¹⁷, R. Sobie²⁸, S. Söldner-Rembold¹⁰, R.W. Springer³⁰, M. Sproston²⁰, K. Stephens¹⁶, J. Steuerer²⁷, B. Stockhausen³, K. Stoll¹⁰, D. Strom¹⁹, P. Szymanski²⁰, R. Tafirout¹⁸, S.D. Talbot¹, S. Tanaka²⁴, P. Taras¹⁸, S. Tarem²², R. Teuscher⁸, M. Thiergen¹⁰, M.A. Thomson⁸, E. von Törne³, S. Towers⁶, I. Trigger¹⁸, E. Tsur²³, A.S. Turcot⁹, M.F. Turner-Watson⁸, P. Utzat¹¹, R. Van Kooten¹², M. Verzocchi¹⁰, P. Vikas¹⁸, E.H. Vokurka¹⁶, H. Voss³, F. Wäckerle¹⁰, A. Wagner²⁷, C.P. Ward⁵, D.R. Ward⁵, P.M. Watkins¹, A.T. Watson¹, N.K. Watson¹, P.S. Wells⁸, N. Vermes³, J.S. White²⁸, B. Wilkens¹⁰, G.W. Wilson²⁷, J.A. Wilson¹, G. Wolf²⁶, T.R. Wyatt¹⁶, S. Yamashita²⁴, G. Yekutieli²⁶, V. Zacek¹⁸, D. Zer-Zion⁸

¹School of Physics and Space Research, University of Birmingham, Birmingham B15 2TT, UK

²Dipartimento di Fisica dell’ Università di Bologna and INFN, I-40126 Bologna, Italy

³Physikalisches Institut, Universität Bonn, D-53115 Bonn, Germany

⁴Department of Physics, University of California, Riverside CA 92521, USA

⁵Cavendish Laboratory, Cambridge CB3 0HE, UK

⁶ Ottawa-Carleton Institute for Physics, Department of Physics, Carleton University, Ottawa, Ontario K1S

5B6, Canada

⁷Centre for Research in Particle Physics, Carleton University, Ottawa, Ontario K1S 5B6, Canada

⁸CERN, European Organisation for Particle Physics, CH-1211 Geneva 23, Switzerland

⁹Enrico Fermi Institute and Department of Physics, University of Chicago, Chicago IL 60637, USA

¹⁰Fakultät für Physik, Albert Ludwigs Universität, D-79104 Freiburg, Germany

¹¹Physikalisches Institut, Universität Heidelberg, D-69120 Heidelberg, Germany

¹²Indiana University, Department of Physics, Swain Hall West 117, Bloomington IN 47405, USA

¹³Queen Mary and Westfield College, University of London, London E1 4NS, UK

¹⁴Technische Hochschule Aachen, III Physikalisches Institut, Sommerfeldstrasse 26-28, D-52056 Aachen, Germany

¹⁵University College London, London WC1E 6BT, UK

¹⁶Department of Physics, Schuster Laboratory, The University, Manchester M13 9PL, UK

¹⁷Department of Physics, University of Maryland, College Park, MD 20742, USA

¹⁸Laboratoire de Physique Nucléaire, Université de Montréal, Montréal, Quebec H3C 3J7, Canada

¹⁹University of Oregon, Department of Physics, Eugene OR 97403, USA

²⁰Rutherford Appleton Laboratory, Chilton, Didcot, Oxfordshire OX11 0QX, UK

²²Department of Physics, Technion-Israel Institute of Technology, Haifa 32000, Israel

²³Department of Physics and Astronomy, Tel Aviv University, Tel Aviv 69978, Israel

²⁴International Centre for Elementary Particle Physics and Department of Physics, University of Tokyo, Tokyo 113, and Kobe University, Kobe 657, Japan

²⁵Brunel University, Uxbridge, Middlesex UB8 3PH, UK

²⁶Particle Physics Department, Weizmann Institute of Science, Rehovot 76100, Israel

²⁷Universität Hamburg/DESY, II Institut für Experimental Physik, Notkestrasse 85, D-22607 Hamburg, Germany

²⁸University of Victoria, Department of Physics, P O Box 3055, Victoria BC V8W 3P6, Canada

²⁹University of British Columbia, Department of Physics, Vancouver BC V6T 1Z1, Canada

³⁰University of Alberta, Department of Physics, Edmonton AB T6G 2J1, Canada

³¹Duke University, Dept of Physics, Durham, NC 27708-0305, USA

³²Research Institute for Particle and Nuclear Physics, H-1525 Budapest, P O Box 49, Hungary

³³Institute of Nuclear Research, H-4001 Debrecen, P O Box 51, Hungary

³⁴Ludwigs-Maximilians-Universität München, Sektion Physik, Am Coulombwall 1, D-85748 Garching, Germany

^a and at TRIUMF, Vancouver, Canada V6T 2A3

^b and Royal Society University Research Fellow

^c and Institute of Nuclear Research, Debrecen, Hungary

^d and Department of Experimental Physics, Lajos Kossuth University, Debrecen, Hungary

^e and Depart of Physics, New York University, NY 1003, USA

1 Introduction

During the years 1990 to 1995 of LEP operation, an integrated luminosity of 163 pb^{-1} has been recorded with the OPAL detector at $\sqrt{s} \approx 91 \text{ GeV}$, corresponding to approximately five million observed Z^0 decays. This large data sample, which contains more than 210000 τ pair events, allows searches for rare decays of the τ lepton with branching ratios down to about 10^{-5} . The high-multiplicity decays of the τ are particularly interesting for a measurement of the τ neutrino mass. Recent examples of such measurements using τ decays into three or five charged particles can be found in references [1, 2]. Taking only kinematical considerations into account, the decay of the τ into twelve pions is possible.

In this note we present a search for τ decays into seven charged particles (7-prong). The HRS Collaboration has published an upper limit of 1.9×10^{-4} on the branching ratio for τ decays into seven charged particles¹, $BR(\tau^- \rightarrow 4\pi^- 3\pi^+ n\gamma \nu_\tau (n \geq 0))$, at the 90% confidence level [3]. The CLEO Collaboration has determined a 95% confidence level upper limit of 1.1×10^{-4} on the branching ratio $BR(\tau^- \rightarrow 3\pi^- 2\pi^+ 2\pi^0 \nu_\tau)$ [4].

2 The OPAL detector

A detailed description of the OPAL detector can be found elsewhere [5]. Sub-detectors which are particularly relevant to the present analysis are described here briefly. The central detector consists of a system of tracking chambers providing charged particle tracking over 96% of the full solid angle inside a 0.435 T uniform magnetic field parallel to the beam axis². Starting with the innermost components, it consists of a high precision silicon microvertex detector which was available from 1991, a precision vertex drift chamber, a large volume jet chamber with 159 layers of axial anode wires and a set of z chambers measuring the track coordinates along the beam direction. The efficiency for separating hits from two different particles in the jet chamber is approximately 80% for distances between two hits of 2.5 mm [6] and drops rapidly for smaller hit distances. The jet chamber also provides energy loss measurements which are used for particle identification.

A lead-glass electromagnetic calorimeter (ECAL) located outside the magnet coil covers the full azimuthal range with excellent hermeticity in the polar angle range of $|\cos\theta| < 0.82$ for the barrel region and $0.81 < |\cos\theta| < 0.984$ for the endcap region. The forward detectors and silicon tungsten calorimeters located at both sides of the interaction point measure the luminosity and complete the geometrical acceptance down to 24 mrad in polar angle.

3 Event simulation

The $e^+e^- \rightarrow \tau^+\tau^-$ Monte Carlo events were generated using KORALZ 4.0 [7]. The dynamics of τ decays to final states with five or fewer charged particles were simulated with the TAUOLA 2.4 decay library [8]. The 7-prong signal events were simulated by modifying the TAUOLA routine describing the decay of the τ into five or more pions to allow up to seven charged pions with either zero ($\tau^- \rightarrow 4\pi^- 3\pi^+ \nu_\tau$) or one neutral pions ($\tau^- \rightarrow 4\pi^- 3\pi^+ \pi^0 \nu_\tau$) in the final state. To determine the efficiency for reconstructing an event with a 7-prong τ decay we generated τ pair events in which the first τ decays according to the standard TAUOLA library and the second one decays into seven charged particles.

We have implemented various phase space models for these 7-prong decays. The standard case assumes an isotropic phase space between the minimum allowed value, equivalent to the sum of the pion masses, and the maximum allowed value, m_τ . To study the effect of the phase space modelling on the final result, we also considered the two extreme cases of a “low” and “high” phase space, that is with a 7-pion invariant mass always

¹References in this paper to specific charge states apply to the charge conjugate states as well.

²The OPAL coordinate system is a right-handed coordinate system which is defined so that the z -axis is in the direction of the electron beam, the x -axis is horizontal and points towards the centre of the LEP ring; θ and ϕ are the polar and azimuthal angles, defined relative to the $+z$ - and $+x$ -axes, respectively.

below or above the value of $1.4 \text{ GeV}/c^2$, which is the mean value of $7m_\pi$ and m_τ . Additionally, we generated 7-prong Monte Carlo events where the invariant mass of the 7-pion system is peaked close to this mean value in a Gaussian manner with a standard deviation of $150 \text{ MeV}/c^2$.

To estimate the background from $e^+e^- \rightarrow \tau^+\tau^-$ events with τ decays into up to five charged particles, we have used a sample of 920000 events generated with KORALZ and TAUOLA. The expected rate of multihadronic background was determined using $e^+e^- \rightarrow q\bar{q}$ events generated with JETSET [9]. The background coming from $e^+e^- \rightarrow e^+e^-$ events was estimated using a sample of simulated $e^+e^- \rightarrow e^+e^-$ events corresponding to a luminosity of 287 pb^{-1} and generated with BABAMC [10]. Contributions from two-photon processes were studied using the PYTHIA [9] and Vermaseren [11] Monte Carlo generators. Background contributions coming from $e^+e^- \rightarrow \mu^+\mu^-$ and four-fermion events are small. They were investigated using the KORALZ and FERMISV [12] event generators, respectively.

All Monte Carlo events were passed through the GEANT [13] simulation of the OPAL detector [14] and were then processed in the same way as the real data.

4 Event preselection

A cone jet algorithm [15] was employed to assign all tracks and electromagnetic clusters to cones with a half opening angle of 35° . We required that exactly two cones with at least one track each were found in the event. Tracks were required to satisfy the following conditions:

- $p_\perp > 0.1 \text{ GeV}/c$, where p_\perp is the momentum component transverse to the beam direction.
- A minimum number of 20 hits in the central jet chamber was required. This restricts the acceptance of the detector for tracks to $|\cos\theta| < 0.965$, where θ is the angle between the track and the beam axis.
- The distance of closest approach of the track to the beam axis must be less than 2 cm and the displacement of the track along the beam axis from the nominal interaction point at the point of closest approach to the beam must be less than 20 cm.

To reject events coming from two-photon interactions, the acollinearity of the two cones was required to be less than 15° , with the direction of each cone given by the momentum sum of all tracks and electromagnetic clusters inside the cone. The momenta of the ECAL clusters were calculated using the energy deposition and the angles of the cluster. The visible energy of each jet is taken as the maximum of the sum of the track momenta and the sum of the ECAL cluster energies associated with that jet. Events were rejected if the sum of the visible energies of the two jets was less than 3% of the centre-of-mass energy. Events with a total visible energy smaller than 20% of the centre-of-mass energy were rejected if the sum of the transverse momenta of the tracks and the sum of the transverse momenta of the electromagnetic clusters were both smaller than 2 GeV. This set of cuts rejects most of the two-photon background. Cosmic ray events were removed using the time-of-flight and the tracking chamber information [16]. Finally, we rejected events where some particles may be lost close to the beam pipe by requiring that the total energy deposit in the forward detectors be less than 2 GeV. We also required $|\cos\theta_{\text{cone}}| < 0.9$ for each of the two cones in the event, where θ_{cone} is the angle between the jet direction and the beam axis. This cut ensures that both jets are located inside the acceptance of the detector.

Only events with a minimum of four tracks were accepted for further analysis. The efficiency for selecting a $\tau^+\tau^-$ event with a 7-prong τ decay after the preselection cuts was $(80.8 \pm 0.5)\%$ according to the Monte Carlo simulation.

5 Selection of 7-prong τ events

At this stage, the largest sources of background, around 55%, come from $e^+e^- \rightarrow q\bar{q}$ events with a low-multiplicity jet, followed by $e^+e^- \rightarrow \tau^+\tau^-$ events with τ decays into five or fewer charged particles ($\approx 33\%$).

These backgrounds were reduced by the following set of cuts. Since approximately 99.9% of the τ leptons decay into one or three charged particles, we required that the number of tracks N_1 in one of the two cones³ is exactly 1 or 3. The absolute value of the sum of the charges of these tracks was required to satisfy $|\sum_{\text{tracks}} q|_1 = 1$. The search for the 7-prong τ decay was performed in the second cone. We required that this contains at least six tracks ($N_2 \geq 6$) and that the absolute value of the sum of the track charges satisfies $|\sum_{\text{tracks}} q|_2 \leq 2$. The distribution of N_2 is shown in Figure 1.

The invariant mass of the tracks from a true 7-prong τ decay must be less than the τ mass. Therefore the invariant mass of the tracks in the second cone, m_2 , calculated using the pion mass for each track, was required to satisfy $m_2 \leq 1.6 \text{ GeV}/c^2$ for cones with six reconstructed tracks and $m_2 \leq 1.9 \text{ GeV}/c^2$ for cones with $N_2 \geq 7$. The cut is lower for the $N_2 = 6$ case since the measured invariant mass of a true 7-prong decay candidate would be smaller due to the missing track. The distribution of m_2 before the cut is shown in Figure 2.

Most of the $q\bar{q}$ events that were not removed by the invariant mass cut were rejected by a cut on the maximum opening angle of any pair of tracks in the two jets. For the first cone we required this angle to be less than 10° ($\alpha_1^{\text{max}} < 10^\circ$) when $N_1 = 3$. For the second cone we required $\alpha_2^{\text{max}} < 8^\circ$. The distribution of α_2^{max} is shown in Figure 2 for the data and for the signal and background Monte Carlo samples after the cuts on m_2 and α_1^{max} have been applied.

Jets likely to contain one or more electrons coming from τ decays with five or fewer tracks and additional tracks from photon conversions or π^0 Dalitz decays were rejected using the energy loss measurement and information on the energy deposit in the electromagnetic calorimeter. For the tracks in the 7-prong candidate cone we have calculated a quantity f_2 , which is the logarithm of the ratio of the χ^2 probability for the measured dE/dx of the track to be consistent with an electron to the probability for the measured dE/dx of the track to be consistent with a pion. If at least 20 dE/dx measurements along the specified track are available, we required f_2 to be less than 5. For the $N_2 = 6$ case this cut was lowered to $f_2 < 3$ to reject the conversion background more effectively. No cut was made for tracks with less than 20 dE/dx measurements or for tracks where both probabilities were smaller than 1%. The distributions of the maximum f_2 is shown in Figure 3. In this figure, the expected signal contribution is normalised assuming a branching ratio equal to the upper limit quoted in reference [3]. To reduce further the background from events containing electrons, we applied the additional cut $(E_{\text{cone}}/P_{\text{cone}})_2 < 0.8$, where E_{cone} is the sum of the energies of all electromagnetic clusters inside the cone and P_{cone} is the sum of the momenta of all tracks associated with the cone.

After all cuts, no event is found in the data. The expected number of background events from all modelled sources is $0.5_{-0.3}^{+1.0}$. The numbers of expected and observed events after each cut are shown in Table 1. The efficiencies for selecting a 7-prong τ event are shown in Table 2 for the signal Monte Carlo samples described in section 3. A branching ratio equal to the upper limit quoted in reference [3] would result in approximately 33 τ pair events containing a 7-prong τ decay being observed in our data sample.

6 Systematic errors

The two sources of systematic errors in this analysis are the uncertainty in the total number of τ pair events, $N_{\tau^+\tau^-}$, and the uncertainty in the 7-prong selection efficiency. We determined $N_{\tau^+\tau^-}$, using the total number of hadronic Z^0 decays and dividing by the ratio of the hadronic and the leptonic branching ratio of the Z^0 corrected for contributions from s-channel photon exchange. The calculated number of τ pair events is $N_{\tau^+\tau^-} = 210680 \pm 1100$. This corresponds to a systematic error of 0.5%.

For the determination of the upper limit on the branching ratio we chose the 7-prong Monte Carlo simulation with the isotropic phase space distribution of the 7-pion system. After all cuts we obtain a selection efficiency of 0.410 for this 7-prong Monte Carlo sample. Among all other 7-prong Monte Carlo simulations described in section 3, only the high phase space model leads to a lower final selection efficiency, which is still consistent with the selection efficiency for the isotropic phase space case. As an estimate of the systematic uncertainty from phase space effects, we therefore use the statistical error of the selection efficiency obtained for the isotropic 7-prong Monte Carlo sample, corresponding to a relative error of 3.9%.

³In the rest of the paper we refer to this as the first cone.

Cut	Number of expected events from MC				OPAL data
	$\tau^+\tau^-$	e^+e^-	$q\bar{q}$	Sum of MC	
Preselection, $N_1 = 1$ or 3 , $N_2 \geq 6$	788 ± 13	83 ± 7	8684 ± 79	9555 ± 81	9593
$ \sum_{\text{tracks}} q _1 = 1$ $ \sum_{\text{tracks}} q _2 \leq 2$	657 ± 12	79 ± 7	8058 ± 76	8794 ± 78	8888
invariant mass cuts	84.6 ± 4.4	20.5 ± 3.4	35.4 ± 5.1	140.5 ± 7.5	131
$\alpha_1^{\text{max}} < 10^\circ$ $\alpha_2^{\text{max}} < 8^\circ$	50.0 ± 3.4	18.2 ± 3.2	0.6 ± 0.6	68.8 ± 4.7	67
dE/dx cuts	3.0 ± 0.8	1.7 ± 1.0	< 1.1	$4.7^{+1.7}_{-1.3}$	4
$(E_{\text{cone}}/P_{\text{cone}})_2$ requirement	0.5 ± 0.3	< 1.1	< 0.6	$0.5^{+1.0}_{-0.3}$	0

Table 1: Number of expected and observed events for a luminosity of 163 pb^{-1} after application of each cut. Only the most important sources of background are included. The number of expected background events is obtained using the Monte Carlo samples (MC) described in the text. The errors shown are statistical only.

To take into account that additional neutral pions may be produced in the final state, we checked differences in the selection efficiencies for the $4\pi^- 3\pi^+ \nu_\tau$ and the $4\pi^- 3\pi^+ \pi^0 \nu_\tau$ decays. Since we did not obtain a lower selection efficiency for the $4\pi^- 3\pi^+ \pi^0 \nu_\tau$ case, we conclude that the branching ratio limit is relatively insensitive to the number of additionally produced neutral pions. The case that kaons may be produced in the final state has been neglected because the corresponding decay modes are expected to be highly suppressed compared to the modes we have considered.

We studied the possible differences in the modelling of the number of reconstructed tracks between data and the Monte Carlo simulation. This comparison was performed using the dE/dx distribution for the tracks in the 7-prong candidate cone. In the OPAL jet chamber, for momenta above $2 \text{ GeV}/c$, single tracks should have a maximum measured dE/dx of $10 \text{ keV}/\text{cm}$ (electrons) and only unresolved double tracks should have a larger dE/dx value. If at least one track with a momentum greater than $2 \text{ GeV}/c$ and a dE/dx value greater than $15 \text{ keV}/\text{cm}$ was found, we conclude that this is due to two tracks that have not been resolved. After applying the preselection and the multiplicity cuts we calculated the fraction f_{res} of 7-prong candidate cones in which such a high dE/dx value was measured. We found that f_{res} is about 2% smaller in the data than in the Monte Carlo simulation. This 2% discrepancy is also found in the low invariant mass region selected with $m_2 < 2 \text{ GeV}$. Relaxing the cut on N_2 , we repeated this study for $N_2 = 4$ and $N_2 = 5$ and obtained similar results. Because a higher efficiency for the data than for the Monte Carlo simulation leads to a systematic error which does not affect the final limit, this effect has been neglected.

The uncertainty arising from the cut on the total charge of the cones was estimated by comparing the ratio of rejected events for data and Monte Carlo simulation when the cut is applied directly after the preselection and the multiplicity cuts, giving a relative uncertainty of 0.7%. For the invariant mass cut and the cut on the maximum angle between any pair of tracks, the systematic uncertainties were estimated by comparing data and Monte Carlo samples selected by requiring after the preselection $N_1 = 1$ and $5 \leq N_2 \leq 7$. The distribution of m_2 after applying these selection criteria is shown in Figure 4. For the two quantities, we obtain a combined relative systematic error of 1.1%. To determine the systematic uncertainties introduced by the cuts on f_2 and $(E_{\text{cone}}/P_{\text{cone}})_2$, we have compared data and Monte Carlo samples selected by requiring after the preselection cuts $N_1 = 1$ and $N_2 \geq 6$ with an additional cut on the invariant mass in the second cone of $m_2 < 3 \text{ GeV}$. For these samples, containing mostly τ pair events, a comparison of the f_2 and $(E_{\text{cone}}/P_{\text{cone}})_2$ distributions between data and the Monte Carlo simulation leads to 7-prong efficiency uncertainties of 0.6% and 1%, respectively. These results are also consistent with those obtained in [17].

Adding the systematic errors in quadrature, the total relative uncertainty of the 7-prong selection efficiency is 4.3% and is dominated by the uncertainty in the modelling of the 7-prong phase space.

Cut	Efficiencies for the 7-prong selection				
	$4\pi^- 3\pi^+ \nu_\tau$				$4\pi^- 3\pi^+ \pi^0 \nu_\tau$
	isotropic	peak	high	low	isotropic
Preselection, $N_1 = 1$ or 3 , $N_2 \geq 6$	0.612±0.015	0.630±0.015	0.660±0.015	0.627±0.015	0.645±0.011
$ \sum_{\text{tracks}} q _1 = 1$ $ \sum_{\text{tracks}} q _2 \leq 2$	0.572±0.016	0.604±0.015	0.618±0.015	0.592±0.016	0.603±0.011
invariant mass cuts	0.472±0.016	0.503±0.016	0.453±0.016	0.513±0.016	0.523±0.012
$\alpha_1^{\text{max}} < 10^\circ$ $\alpha_2^{\text{max}} < 8^\circ$	0.447±0.016	0.480±0.016	0.444±0.016	0.479±0.016	0.493±0.012
dE/dx cuts	0.419±0.016	0.453±0.016	0.416±0.016	0.451±0.016	0.443±0.012
$(E_{\text{cone}}/P_{\text{cone}})_2$ requirement	0.410±0.016	0.446±0.016	0.404±0.016	0.445±0.016	0.420±0.012

Table 2: *Efficiencies after each cut for the selection of a 7-prong τ event as obtained from the different Monte Carlo simulations described in section 3. The errors shown are statistical only.*

The reliability of the predicted background rate for $e^+e^- \rightarrow e^+e^-$ events and $e^+e^- \rightarrow \tau^+\tau^-$ events with τ decays into up to five charged particles was effectively tested using the distribution of the total electromagnetic energy deposited in the second cone before the dE/dx cuts, as shown in Figure 4. Good agreement is observed between the data and the Monte Carlo simulation. The number of expected multihadronic background events has been obtained using the JETSET prediction which has been scaled down by 10-20% (depending on the exact fragmentation parameters and hadronic branching ratios used in each JETSET sample) to fit the data for events with $N_1 = 1$ or 3 and $10 \leq N_2 \leq 15$. To check the reliability of the $e^+e^- \rightarrow q\bar{q}$ background prediction, we have repeated the analysis without applying the dE/dx and $(E_{\text{cone}}/P_{\text{cone}})_2$ cuts and reversing the cut on α_1^{max} . This selects an almost pure sample of multihadronic decays in the region where the signal is expected. Within the limited statistics available, good agreement is found between the data and the Monte Carlo prediction: 5 events are observed in data and 4.8 ± 1.8 are predicted by the simulation.

7 Results

Using data collected with the OPAL detector at LEP at centre-of-mass energies on or near the Z^0 resonance, we have searched for decays of the τ lepton into seven or more charged particles. No candidate events were observed. An upper limit on the branching ratio is obtained using the calculated number of τ pair events, $N_{\tau^+\tau^-} = 210680 \pm 1100$, and the detection efficiency of $(41.0 \pm 1.8)\%$ according to

$$BR(\tau^- \rightarrow 4\pi^- 3\pi^+ n\gamma \nu_\tau (n \geq 0)) < \frac{3.0}{2 \cdot N_{\tau^+\tau^-} \cdot 0.410} \quad (1)$$

The total relative systematic error of 4.3% was included in the manner described in reference [18]. We obtain the upper limit on the branching ratio of

$$BR(\tau^- \rightarrow 4\pi^- 3\pi^+ n\gamma \nu_\tau (n \geq 0)) < 1.8 \times 10^{-5} \quad (2)$$

at the 95% confidence level. This is equivalent to an upper limit of 1.4×10^{-5} at the 90% confidence level. An improvement of more than one order of magnitude is achieved compared to the only previously published result [3].

Acknowledgements:

We particularly wish to thank the SL Division for the efficient operation of the LEP accelerator and for their continuing close cooperation with our experimental group. We thank our colleagues from CEA, DAPNIA/SPP, CE-Saclay for their efforts over the years on the time-of-flight and trigger systems which we continue to use. In addition to the support staff at our own institutions we are pleased to acknowledge the

Department of Energy, USA,

National Science Foundation, USA,

Particle Physics and Astronomy Research Council, UK,

Natural Sciences and Engineering Research Council, Canada,

Israel Science Foundation, administered by the Israel Academy of Science and Humanities,

Minerva Gesellschaft,

Benozziyo Center for High Energy Physics,

Japanese Ministry of Education, Science and Culture (the Monbusho) and a grant under the Monbusho International Science Research Program,

German Israeli Bi-national Science Foundation (GIF),

Direction des Sciences de la Matière du Commissariat à l'Energie Atomique, France,

Bundesministerium für Bildung, Wissenschaft, Forschung und Technologie, Germany,

National Research Council of Canada,

Hungarian Foundation for Scientific Research, OTKA T-016660, T023793 and OTKA F-023259.

References

- [1] OPAL Collaboration, G. Alexander et al., *Z. Phys.* C72 (1996) 231.
- [2] OPAL Collaboration, R. Akers et al., *Z. Phys.* C65 (1995) 183;
ALEPH Collaboration, D. Buskulic et al., *Phys. Lett.* B349 (1995) 585.
- [3] HRS Collaboration, B.G. Bylsma et al., *Phys. Rev.* D35 (1987) 2269.
- [4] CLEO Collaboration, D. Gibaut et al., *Phys. Rev. Lett.* 73 (1994) 934.
- [5] OPAL Collaboration, K. Ahmet et al., *Nucl. Instr. Meth.* A305 (1991) 275;
P.P. Allport et al., *Nucl. Instr. Meth.* A324 (1993) 34;
P.P. Allport et al., *Nucl. Instr. Meth.* A346 (1994) 476.
- [6] O. Biebel et al., *Nucl. Instr. Meth.* A323 (1992) 169.
- [7] S. Jadach, B.F.L. Ward and Z. Wąs, *Comp. Phys. Comm.* 79 (1994) 503.
- [8] S. Jadach, Z. Wąs, R. Decker and J.H. Kühn, *Comp. Phys. Comm.* 76 (1993) 361.
- [9] T. Sjöstrand and M. Bengtsson, *Comp. Phys. Comm.* 43 (1987) 367;
M. Bengtsson and T. Sjöstrand, *Phys. Lett.* B185 (1987) 435;
M. Bengtsson and T. Sjöstrand, *Nucl. Phys.* B289 (1987) 810;
T. Sjöstrand, *Comp. Phys. Comm.* 82 (1994) 74.
- [10] F.A. Berends, R. Kleiss and W. Hollik, *Nucl. Phys.* B304 (1988) 712.
- [11] R. Bhattacharya, J. Smith and G. Grammer, *Phys. Rev.* D15 (1977) 3267;
J. Smith, J.A.M. Vermaseren and G. Grammer, *Phys. Rev.* D15 (1977) 3280.
- [12] J. Hilgart, R. Kleiss and F. Le Diberder, *Comp. Phys. Comm.* 75 (1993) 191.
- [13] R. Brun et al., *GEANT3 User's Guide*, CERN DD/EE/81-1 (1989).
- [14] J. Allison et al., *Nucl. Instr. Meth.* A317 (1992) 47.
- [15] OPAL Collaboration, G. Alexander et al., *Z. Phys.* C52 (1991) 175.
- [16] OPAL Collaboration, R. Akers et al., *Z. Phys.* C66 (1995) 543.
- [17] OPAL Collaboration, R. Akers et al., *Z. Phys.* C68 (1995) 555.
- [18] R. D. Cousins and V. L. Highland, *Nucl. Instr. Meth.* A320 (1992) 331.

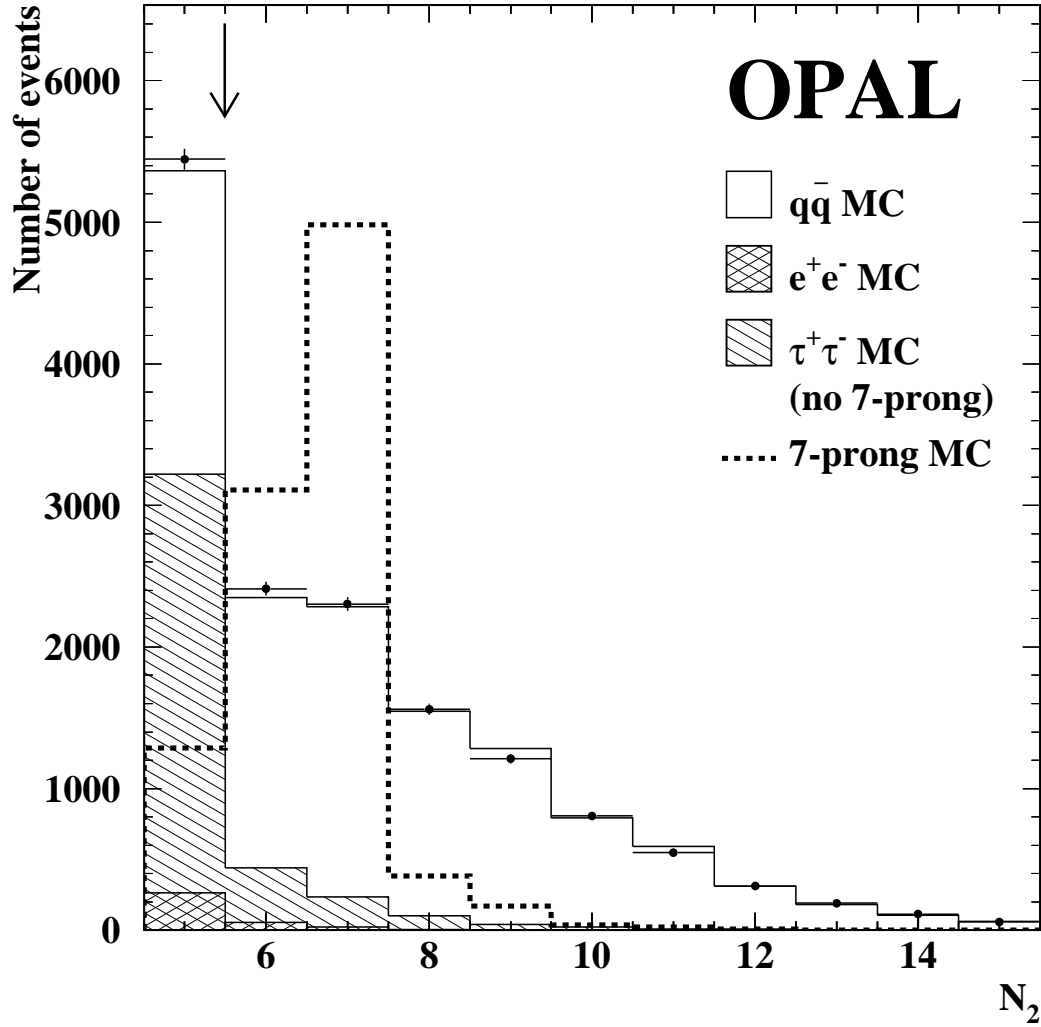


Figure 1: *Distribution of the number of tracks, N_2 , in the second cone after relaxing the cut to $N_2 \geq 5$. An arbitrary normalisation is used for the 7-prong signal Monte Carlo simulation. The other histograms show the contributions from the various background Monte Carlo samples. The points are the data. The arrow indicates the position of the selection cut.*

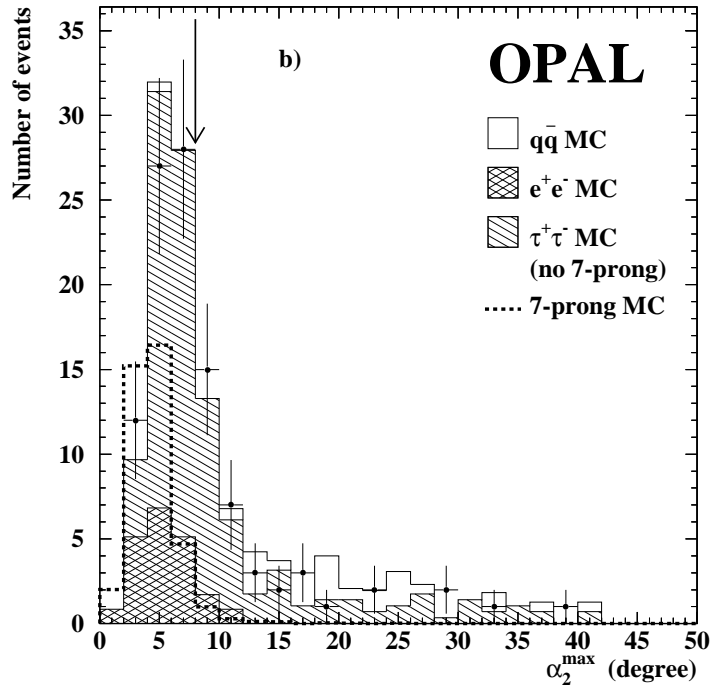
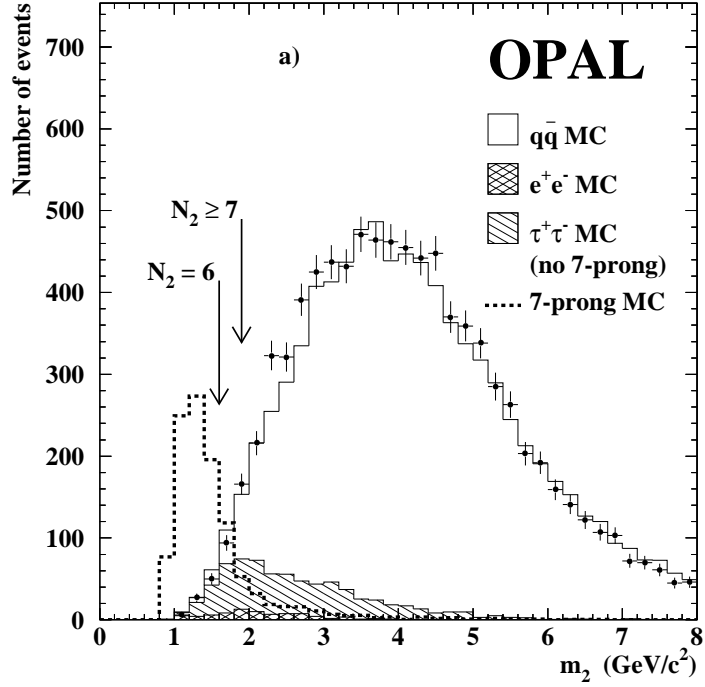


Figure 2: Distribution of m_2 before the invariant mass cut (a) and of α_2^{\max} after the cuts on m_2 and α_1^{\max} (b). An arbitrary normalisation is used for the 7-prong signal Monte Carlo simulation. The other histograms show the contributions from the various background Monte Carlo samples. The points are the data. The arrows indicate the positions of the selection cuts.

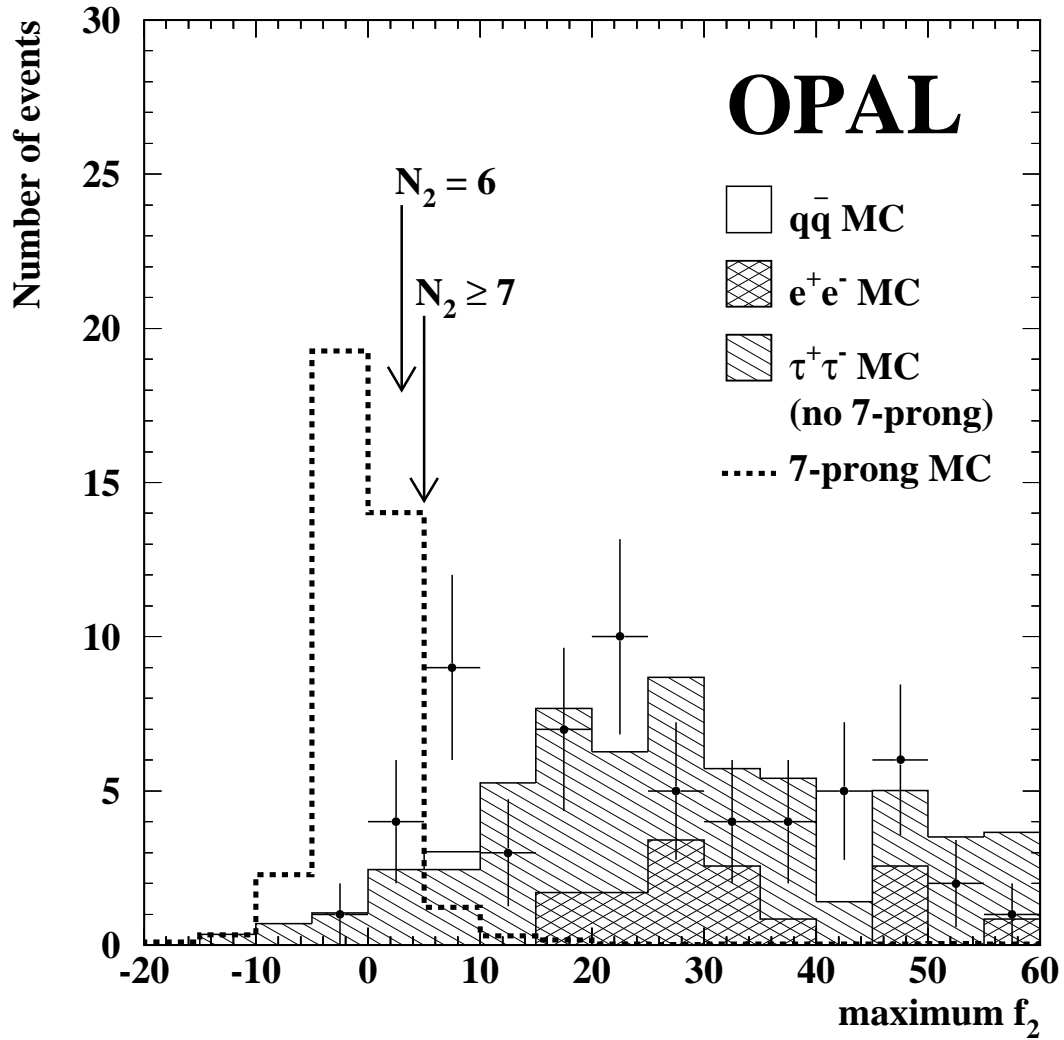


Figure 3: *Distribution of the maximum f_2 before the dE/dx cuts. The 7-prong signal Monte Carlo simulation was normalised assuming a branching ratio equal to the upper limit quoted in Ref. [4]. The other histograms show the contributions from the various background Monte Carlo samples. The points are the data. The arrows indicate the position of the selection cuts.*

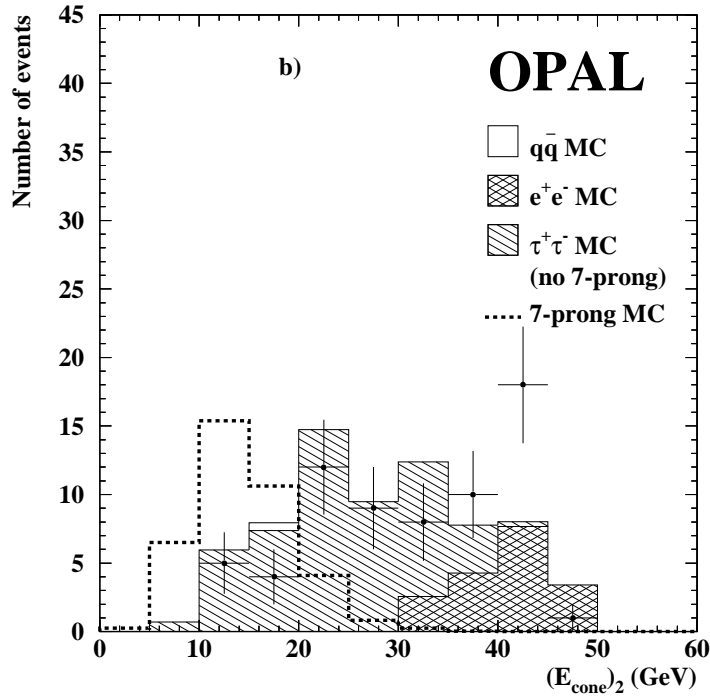
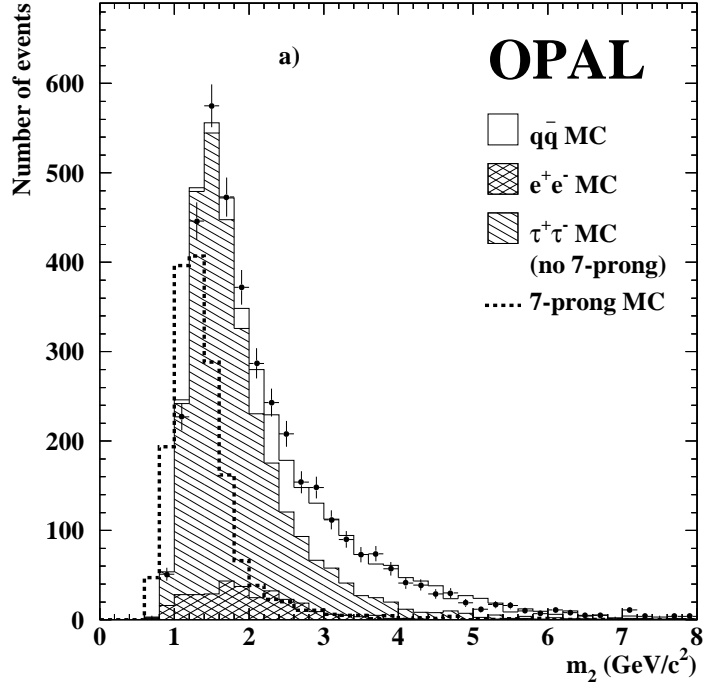


Figure 4: Distribution of m_2 selected by requiring after the preselection $N_1 = 1$ and $5 \leq N_2 \leq 7$ (a) and of the total electromagnetic energy deposited in the 7-prong candidate cone before the dE/dx cuts (b). An arbitrary normalisation is used for the 7-prong signal Monte Carlo simulation. The other histograms show the contributions from the various background Monte Carlo samples. The points are the data.